



# A gas-flow funnel system to quantify advective gas emission rates from the subsurface

Alexander Lübben<sup>1</sup> · Carsten Leven<sup>1</sup>

Received: 22 November 2021 / Accepted: 2 July 2022 / Published online: 29 July 2022  
© The Author(s) 2022

## Abstract

The estimation of greenhouse gas emission rates from the subsurface into the atmosphere is an important part of climate-related research activities and associated efforts concerning the global carbon cycle. For the direct quantification of gas emission rates from the subsurface to the atmosphere a large variety of gas detection and flux quantification techniques exists. With the goal of measuring advective CO<sub>2</sub> gas exhalations circumventing limitations of available systems such as e.g. accumulation-chamber systems or eddy-flux covariance methods, we developed a simple, robust, and low-cost gas-flow funnel system. The device allows for the continuous measurement of mass flow rates with a free, unrestricted gas flow from advectively dominated gas exhalation spots. For the design of the gas-flow funnel we used custom-made, though easy-to-produce components, and sensors that are typically already available when working at such sites. Our general design can easily be applied at sites with focused, advectively driven gas exhalation like volcanic areas, shale-gas seeps, landfills, and open boreholes. For the proof-of-concept we tested the system during three field campaigns at a site with natural CO<sub>2</sub>-bound emissions associated with a geologic fault in southwestern Germany. The measurements showed to be comparable and repeatable throughout the three campaigns, and are consistent with findings from other field sites with comparable CO<sub>2</sub> exhalations.

**Keywords** Gas monitoring · Advective gas fluxes · CO<sub>2</sub> exhalations · Mofette · Greenhouse gas

## Introduction

The quantification of gas fluxes is a main task in environmental research related to gas emissions. Especially, the estimation of greenhouse gas emission rates from the subsurface into the atmosphere is an important part of climate-related research activities and associated efforts concerning the global carbon cycle. In this regard, research focuses on gas emissions from subsurface reservoirs of carbon dioxide (CO<sub>2</sub>) from geological sources or (leaking) carbon capture and storage (CCS) sites (Bigi et al. 2014; Dixon and Romanak 2015; Holloway et al. 2007; Jones et al. 2014; Jung et al. 2015; Kis et al. 2017); on methane emissions from melting permafrost or related to volcanic activity (Etiope and Klusman 2002; Gal et al. 2019; Kang et al. 2014); and on sulfur dioxide (SO<sub>2</sub>) and hydrogen sulfide (H<sub>2</sub>S) emissions which might also considerably contribute to volcanic

exhalations (O'Dwyer et al. 2003; Symonds et al. 2018; Werner et al. 2013). The monitoring of radon fluxes can serve investigations related to earthquakes and/or volcanic eruptions in volcanic areas, and the detection of tectonic fault structures (Schuetze et al. 2012; Steinitz et al. 2007; Zafrir et al. 2016). Gas-flux monitoring is also indicated for assessing e.g. natural attenuation processes at contaminated sites or the environmental impact of abandoned landfills on sensitive receptors (Cardellini et al. 2003; Heggie and Stavropoulos 2018; Jovanov et al. 2018; Scheutz and Kjeldsen 2019). Furthermore, fugitive emissions from abandoned oil and gas wells might be an important pathway for gases from subsurface sources and gas-flux measurements are essential to evaluate their contribution to the global gas exchange processes (Boothroyd et al. 2016; El Hachem and Kang 2022; Kang et al. 2014; Levintal et al. 2020; Neepser 2003).

For the quantification of gas emissions from the subsurface to the atmosphere a large variety of gas detection and flux quantification techniques exists, e.g. based on optical and remote sensing methods (e.g., Feitz et al. 2018; Sauer et al. 2014). In the following we highlight three prominent methods which are regularly used for the quantification of

✉ Carsten Leven  
carsten.leven-pfister@uni-tuebingen.de

<sup>1</sup> Department of Geosciences, University of Tübingen,  
Schnarrenbergstr. 94-96, 72074 Tübingen, Germany

CO<sub>2</sub> fluxes at the direct interface between the subsurface and the atmosphere:

Accumulation-chamber systems (“closed-chamber systems”) consist of a chamber, a rigid collar, a pump, and a gas analyzer. The collar is pushed into the soil to ensure an air-tight connection to the soil and the chamber is placed on top. By this, gas emanating from the subsurface can accumulate in the closed chamber and the measurement of the gas accumulation within the chamber, i.e., increase in gas concentration over a certain time period, is used to determine the mass flux (Amonette and Barr 2009; Chiodini et al. 1998; Elío et al. 2012). The gas analyzers are equipped with gas-specific sensors typically covering a particular concentration span depending on the expected gas emanation concentrations. In the case of high gas emissions, a strong increase in gas concentration within the relatively small chambers occurs however over a very short period of time. Such closed-chamber systems are well-established and widely used since a long time for the estimation of CO<sub>2</sub> fluxes but also for other gases, e.g., methane or helium (Boodoo et al. 2017; Cardellini et al. 2003; Chiodini and Frondini 2001; Gal et al. 2018; Lewicki et al. 2003; Shimoike et al. 2002; Sorey et al. 1998). Limitations of such systems might be, besides relatively high equipment costs, the comparably small areas that can be covered with the chambers on the order of a few decimeters. Moreover, the applicability of such chambers might be limited for the quantification of advective gas fluxes, for which high gas concentrations lead to fast gas accumulation, and / or high gas emanation, i.e., advective volume fluxes lead to an overpressure in the closed chamber. First might be problematic due to long response times, especially of nondispersive infrared CO<sub>2</sub> sensors (typically with response times of up to 30 s and more), and latter might lead to a bypassing of gas of the closed chamber. Therefore, these systems are preferably used to determine diffusive gas fluxes with slow gas accumulation in the chamber, and furthermore chambers are moved between sampling points to cover large areas (Evans et al. 2002; Kis et al. 2017).

For the survey of large-scale CO<sub>2</sub> exhalations the eddy-covariance (EC) method is often advantageous to determine the gas flux between the subsurface and the atmosphere by quantifying the turbulent, vertical exchange of gases, water vapor, and energy (e.g., Baldocchi 2003). Such micrometeorological systems usually include an anemometer to measure the wind speed along three axes and several sensors to determine the air temperature, and concentrations of the respective gases, e.g. water vapor, CO<sub>2</sub>, methane (Moncrieff et al. 1997). However, EC measurements might be biased by site specific factors, such as a heterogeneous topography and vegetation, and changing weather conditions (Baldocchi 2014) resulting in incorrect flux estimates. Furthermore, EC measures averaged vertical gas exchange rates and the

calculation of mass fluxes requires extensive processing of the data. The method is suitable to determine gas fluxes from many small point sources when they appear in large numbers and can be considered as an effective areal source. However, the method is limited when the sources are distributed over an area of certain extent and need to be differentiated, although there have been several attempts to improve the estimating for point sources (Coates et al. 2017; Dumortier et al. 2019).

Boreholes and wells provide direct access to the subsurface and can be used for gas flux measurements by quantifying the air mass movement within boreholes (Levintal et al. 2018). Here it is assumed that the considered gas (e.g., CO<sub>2</sub>) has a constant concentration at a certain depth within a borehole under static conditions and may be different at other depths. However, movement of the gas phase within the borehole may be triggered by barometric pumping (Forde et al. 2019) or due to changes in the density, i.e., the concentration gradient within the borehole caused by temperature variations, or gas supply from a deeper reservoir or prior to earthquakes (Zafirir et al. 2020). Resulting temporal changes in gas concentration can be used to determine the corresponding gas mass fluxes (Levintal et al. 2020). Alternative approaches to flux measurements within open boreholes use chambers similar to the above-discussed accumulation chambers to seal off the wellhead to capture the complete fugitive emissions from a borehole (Kang et al. 2014).

In addition to the sometimes high costs, the methods presented above are either not completely suitable for advective gas exhalations (closed chamber systems) or are not sufficiently mobile and depend on specific site conditions (EC method), or require boreholes and sensors within a borehole. For the measurement of advective gas fluxes from a point source, such as mofettes, vents, etc., it is also important to capture the total amount of the emanating gas without disturbing the pressure conditions at an exhalation point. Specifically, the use of systems working with sealed or insufficiently vented chambers would result in the formation of a back pressure, which would cause changes in gas density and might lead to deficient estimates of emission rates or fluxes.

With the goal of measuring advective CO<sub>2</sub> gas exhalations circumventing the above-described limitations, we developed a simple, robust, and low-cost measuring device that allows for the continuous measurement of mass flow rates from advectively dominated gas exhalation spots, which we present here. Our approach relies on a free, unrestricted gas outflow, which is an important difference to the above-mentioned systems based on the closed-chamber principle. We use custom-made, though easy-to-produce components, and sensors that are typically already available when working at such sites. Also, the approach is robust enough to be deployed in harsh environments and remote areas with restricted accessibility. To prove the concept, we

tested the system at a site that is characterized by natural CO<sub>2</sub> exhalations.

## Conceptual design

The system described here was originally designed to determine the gas flux of advective CO<sub>2</sub> exhalations at a site in southwestern Germany with natural CO<sub>2</sub> emissions associated with a geologic fault (Lübben and Leven 2018). Considering the limitations of available systems as presented in the introduction, it became clear that none of the above-discussed approaches was suitable at the site for determining mass fluxes at the advectively-driven exhalation points, either due to elevated exhalations pressures (preventing the use of closed-chamber systems), heterogeneous vegetation and topography (preventing the use of EC flux or optical and remote sensing methods), and all boreholes from a century-long industrial CO<sub>2</sub> use were closed and abandoned. We defined technical requirements for the design of an adapted CO<sub>2</sub> flux method for our given site as following:

- Suitable for the measurement of advective gas emission rates from point sources without disturbing the pressure conditions of the emanating gas, i.e., allowing a free outflow of gas without the formation of a pressure accumulation during the measurement.
- Applicable and adaptable to different sizes of exhalation points and measurement environments, e.g. for high and low emission rates, pressures, and gas concentrations.
- Suitable for the acquisition of time-series of at least several hours to days with low power consumption, for which batteries or small solar panels should suffice.
- Easy-to-built with a simple design and a low budget.
- Use of devices that are readily available when working in such environments.
- Mobile enough to easily install and move between sites and measurement locations, i.e., light weight and small in size to allow for easy transport over long distances without the need of vehicles for transport, and setup and operation by only one person.

For a free gas outflow and under the assumption of an ideal gas, the volume of gas  $V$  [m<sup>3</sup>] is expressed following the ideal gas law with

$$V = \frac{nRT}{p} \quad (1)$$

where  $n$  is the amount of gas molecules [mol],  $R$  as the ideal gas constant [m<sup>3</sup> bar mol<sup>-1</sup> K<sup>-1</sup>],  $T$  as the absolute temperature [K], and  $p$  as the gas pressure [bar]. The gas volume advectively released from a point source is a direct function

of the gas flow velocity  $v$  [m/s] and the cross-sectional area  $A$  [m<sup>2</sup>] through which the gas flow occurs in the time  $t$  [s]

$$V = vAt \quad (2)$$

With this, the gas flow rate  $\phi$  [mol/s] can accordingly be expressed as

$$\phi = \frac{n}{t} = \frac{pvA}{RT} \quad (3)$$

Depending on the type of gas concentration measurements, it might be more convenient to express the gas flow rate in terms of gas mass  $m$  [g] with

$$m = nMc \quad (4)$$

where  $M$  is the molar gas mass  $M$  [g/mol], and the volumetric gas concentration  $c$  [vol%], thus the gas mass flow rate  $\dot{m}$  [kg/s] is given by

$$\dot{m} = \frac{pcvA}{R_s T} \quad (5)$$

with the specific gas constant  $R_s$  [J kg<sup>-1</sup> K<sup>-1</sup>] which is e.g. 188.92 J kg<sup>-1</sup> K<sup>-1</sup> for CO<sub>2</sub>.

To measure the volumetric flow rate of a gas emanating from a point source according to (5), a chamber with an open outlet of known geometry, i.e. open area  $A$  is required at which the velocity  $v$  of the streaming gas, its temperature  $T$ , pressure  $p$ , and the gas concentration  $c$  can be measured. To capture the gas emanating from a point source, we utilize a funnel-like chamber with a base area large enough to cover the point source (in our case CO<sub>2</sub> mofettes of different sizes) and to collect all emanating gas from the point source. Free gas outflow occurs through a chimney with known geometry. The diameter of the chimney has to be sufficiently large to guarantee unrestricted and laminar outflow of the gas, though the diameter should also be small enough to generate a sufficient gas flow velocity to allow for a reliable gas velocity measurement.

## Our realization of the gas-flow funnel

Based on the above-described requirements and conditions, we constructed a modular system shown in Fig. 1, in the following addressed as “gas-flow funnel”: It consists of (i) a gas-tight hood to collect the emanating gas from the point-source, (ii) a chimney to focus and quantify the amount of emanating gas, and (iii) several ports in the hood and chimney allowing the installation of sensors for measurements of pressure, temperature, gas flow velocity, and gas concentration as well as gas sampling. The hood consists of a half metal barrel, in which we cut a central opening of several centimeters in diameter for the chimney and several

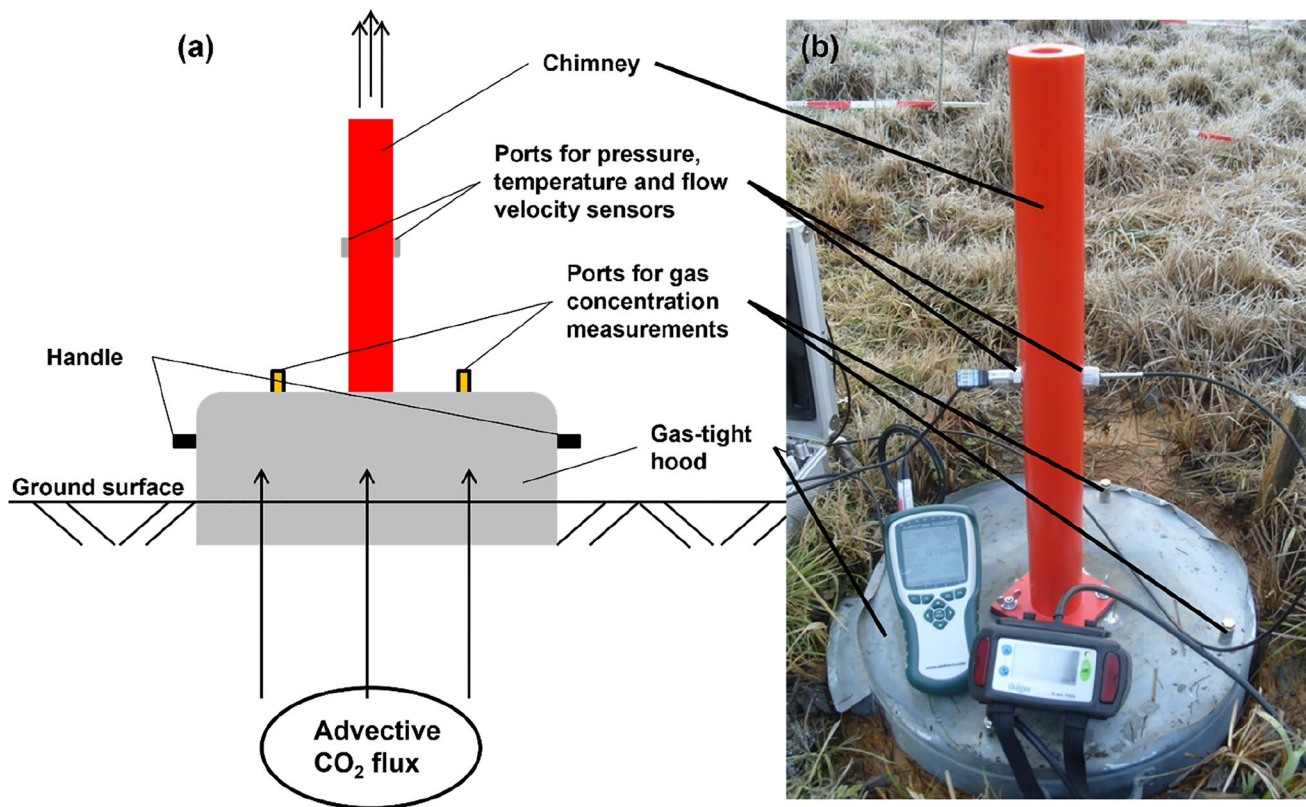


**Fig. 1** **a** Sketch of the "gas-flux funnel" to determine mass flux from a CO<sub>2</sub> point source, and **b** photograph during its field application to quantify the CO<sub>2</sub> mass flux from a mofette including a gas detector,

gas velocity, temperature and pressure sensors with data acquisition device. The dimensions of the system are given in Table 1

smaller openings serving as access ports close to the rim. The geometries of the gas-flow funnel used at our test site are given in Table 1. The chimney, consisting of a 600 mm long PVC pipe with a nominal inner diameter of 26.5 mm, is attached to the central opening of the hood, and in the middle section of the chimney two openings are used for placing the gas flow and pressure sensors on opposite sides. The gas sensor (in our case for CO<sub>2</sub>) is installed in one of the ports on top of the hood and not in the chimney to not disturb the gas flow measurements there. The barrel used as hood has a relatively thin metal wall resulting in sharp edges, which helps to easily push the hood into the ground, inducing only small disturbances of the soil, and creating a tight connection to the surrounding soil. Due to the modular setup of the gas-flow funnel, all components can be simply assembled at

the measurement location within a few minutes and disassembled for easy transport between sites.

### Sensors and data acquisition

For our setup, we used a hot-wire anemometer (Ahlborn Mess- und Regelungstechnik GmbH, Holzkirchen, Germany) for measuring the flow velocity of the streaming gas within in the chimney. The use of a hot-wire anemometer has the advantage, e.g. over cup anemometers that the sensor itself only disturbs the free gas flow as little as possible. For that reason, we assume that a potential disturbance occurring close to the sensors within the cylinder has a negligible influence on the measured parameters itself. Since the flow velocity of the streaming gas is influenced by pressure and

**Table 1** Specifications of the components of the gas-flow funnel

Component	Material	Length/height	Inner diameter	Remarks
Chimney	PVC	600 mm	26.5 mm	Gas-tight connection to the gas-tight hood and measurements ports, wall thickness approx. 20 mm
Gas-tight hood	Metal	200 mm	400 mm	Small wall thickness (5 mm) and sharp edge, measurement ports in top

temperature, the anemometer system also acquires data for temperature and pressure compensation. However, an additional pressure sensor is used for the calculation of mass flow rates presented here. All sensors are installed in the chimney of the gas-flow funnel with air-tight couplings (grey compression fittings at the chimney in Fig. 1b). The pressure sensor does not reach into the chimney to prevent disturbance of the gas flow while the gas flow sensor has to be placed in the middle of inner part of the chimney. The specifications of the sensors are given in Table 2.

To test the reliability of the flow velocity measurement within the chimney, we conducted control tests in the lab, in which we flushed pure CO<sub>2</sub> gas through the chimney with different flow rates, which were controlled by a valve and a variable-area flowmeter. The control tests indicated differences between the applied flow rate and the measured flow rate in the chimney in the range of 2 and 5% of the measurement value, while we expect that the inaccuracy of the variable-area flowmeter mainly explains the differences between the applied and measured rates.

It should also be noted that the measurement range of the anemometer and the inner diameter of the chimney have to be selected according to the expected gas flow velocities so that accurate gas velocity measurements can be achieved, and turbulent flow conditions with too high Reynolds numbers can be avoided within the chimney. Also, to generate an ideal gas flow profile for an accurate measurement within the chimney, the upstream and downstream section from the measurement point have to have a minimum length. For a straight pipe the minimum distance to the sensor is typically defined as six to ten times the pipe diameter for the upstream section (e.g., DIN EN 12599 2012), i.e., in this case approx. 160 to 270 mm, which is why we used a chimney length of 600 mm and placed the anemometer at half of the length.

The data from these sensors was acquired and stored with a data logger with a low power consumption so that a standard 12 V battery (7.2 Ah) was sufficient for acquiring data sets over several days.

The measurement of gas emission rates focused on CO<sub>2</sub> emanations for which a respective gas detector (Dräger Safety AG & Co. KG, Lübeck, Germany) was used. The gas detector is connected to a port on top of the hood via a rubber tubing. Due to the very high CO<sub>2</sub> concentrations, a sensor with a full-scale range of 100 vol% had to be chosen (Table 2), though it is advisable to also select the measurement range of the sensor according to the expected gas concentration for accurate measurements.

### Installation of the gas-flow funnel

The gas-flow funnel is placed gas tight over the gas exhalation point in a way that all emanating gas is caught and directed through the chimney. When placed over an exhalation point, the open bottom of the hood is pushed into the surrounding soil. To tighten the connection, the adjacent soil can be pressed against the hull of the hood after placement. Furthermore, to verify that all gas from the exhalation site is caught by the hood, the soil surface around the hood can be covered with water. The absence of gas bubbles proves a gas tight connection of the hood to the soil surface. If necessary, sealing can also be improved by adding wet bentonite or other plastic soil material.

As discussed above, the diameter of the chimney needs to be selected according to the amount of emanating gas, so that (i) no backpressure is generated in the gas-flow funnel which could lead to a lateral leakage alongside the measuring setup or along preferential flow paths in the soil (e.g., along plant roots or earthworm tunnels); and (ii) laminar gas outflow is guaranteed but also a sufficient gas flow velocity

**Table 2** Manufacturers' specifications of sensors used for mass flux determination

Measured variable	Sensor/device	Measuring range	Resolution	Accuracy	Response time
Temperature	Ahlborn FVAD35 hot-wire anemometer	- 20... +70 °C	0.1 K	0.7 °C	10 s
Gas flow velocity		0.08...2.0 m/s	0.001 m/s	(0.04 m/s + 1% of MV) 0.5% of MV/°C	
Pressure	Ahlborn FDA602L3A pressure transducer	< 2.5 bar (absolute)	1.0 mbar	1.0% of MV	< 5 ms
CO <sub>2</sub> gas concentration	Dräger X-am 7000	< 100 vol%	0.2 vol% for < 25 vol% 1 vol% for 25...49 vol% 2 vol% for ≥ 50 vol%	≤ 1 vol% CO <sub>2</sub> ≤ 5% MV	< 10 s
Air pressure	DAVIS Vantage 2 PRO	0.8 – 1.08 bar	0.1 mbar	1.7 mbar	1 min <sup>a</sup>
Air temperature		- 40... +60 °C	0.1 K	0.5 °C	10 s <sup>a</sup>

MV = measured value

<sup>a</sup>Read out intervals

is generated for a reliable gas velocity measurement. The formation of a back pressure is typically observable in the pressure data e.g. by strong increases and/or fluctuations, and distinct deviations from the ambient air pressure.

Also, to protect the field equipment from being damaged by adverse weather conditions (e.g. heavy rain, strong heat or frost) and prevent skewed measurements, e.g. by strong heating of sensors, the equipment should be placed under protective installations (e.g. tent / pavilion / tarp).

## Proof of concept, measurement results, and discussion

To show the applicability of the gas-flow funnel and its performance, we present data collected during three campaigns carried out at different seasons at a site in the Upper Neckar valley in southwestern Germany. The area is known for numerous naturally occurring CO<sub>2</sub> springs, which were industrially used for almost a century. The CO<sub>2</sub> exhalations occur most prominently as mofettes, i.e., locally focused, cold and dry CO<sub>2</sub> exhalation with concentrations continuously above 98 vol%, appearing as almost round holes or depressions at the ground surface. Gas measurements in the past performed in the shallow subsurface (soil gas) as well as directly above mofettes yielded CO<sub>2</sub> concentrations between a few vol% (for areas with diffusion-dominated CO<sub>2</sub> migration) and up to 100 vol% (for advectively-driven exhalation spots, esp. mofettes). A detailed description of the site is given in Lübben and Leven (2018).

### Field site campaigns

For the gas-flux measurements presented here, we selected the largest, accessible mofette at the site with an almost round shape and a diameter of approximately 25 cm—see also Fig. 2a in Lübben and Leven (2018). Three measurement campaigns were carried out at the partly water-filled mofette over several days during different seasons. Detailed information on the campaigns is given in Table 3, and the measurement conditions during the campaigns are described with the results in the following.

For each campaign the gas-flow funnel was placed over the mofette as described in the previous section, while it was sufficient to press the hood into the soil by approx. 5–10 cm to ensure a gas-tight connection. During all campaigns the CO<sub>2</sub> concentration of the emanating gas was determined at the beginning, at the end, and repeatedly throughout the campaigns. The measured concentrations were consistently at 98 vol% or above independent of changing atmospheric conditions as also previous measurements at the site confirm (see also Table 1 in Lübben and Leven, 2018). For simplicity, we therefore assume in the following a CO<sub>2</sub>

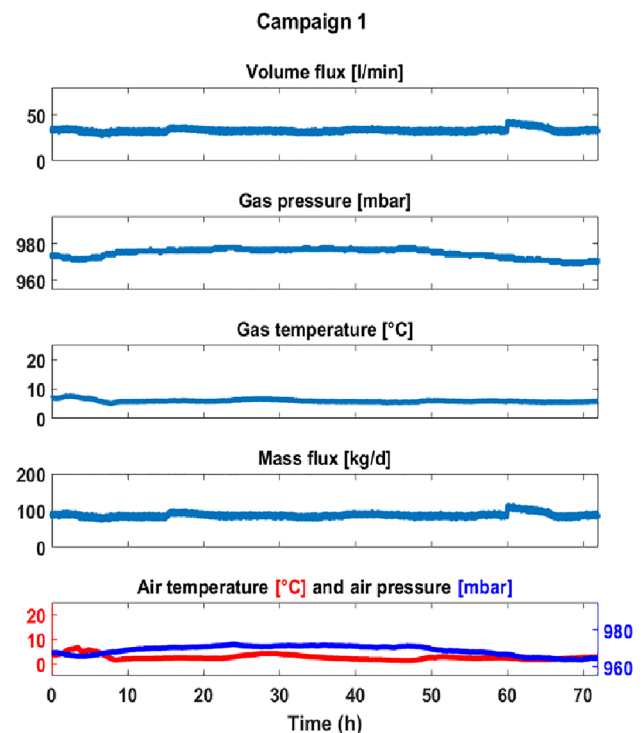


**Fig. 2** Results from field campaign 1. Top row shows the gas volume flux in l/min, the second and third row present gas pressure [mbar] and temperature [°C] and the fourth row gives the calculated CO<sub>2</sub> mass flux [kg/d]. The bottom row shows the meteorological parameters air temperature [°C] and pressure [mbar]

concentration of 100 vol% and other gas concentrations to be negligible. Also, during all campaigns we recorded the atmospheric conditions by a weather station located at the field site (Vantage 2 PRO, DAVIS, California, USA).

Figures 2 and 3 show the results obtained from the individual campaigns with the gas volume fluxes, gas pressures and temperatures measured within the chimney and the resulting calculated CO<sub>2</sub> mass flow rates. Here we also note that the CO<sub>2</sub> concentrations were repeatedly and sporadically measured during the individual campaigns. Statistics of the measured and determined parameters are given in Table 4.

### Campaign 1

The measurements of the first campaign started in the late morning and took place over a period of three days without precipitation during late fall with comparably small changes in air temperature of up to around 5 °C with an average temperature of 2.6 °C. The measured gas temperature ranged between 5.0 and 7.7 °C with a mean value of 6.1 °C (Table 4).

The gas pressure varied slightly between 969 and 978 mbar over the measurement period, while the air pressure was only slightly but consistently lower in the range of

**Table 3** Measurement campaigns

	Campaign 1	Campaign 2	Campaign 3
Season	Late fall	Early spring	Late summer
Duration of campaign	72 h	95 h	102 h
Starting time of campaign	10:30 h	16:00 h	11:20 h
Recording interval gas parameters	5 and 10 s	10 and 20 s	15 s
Recording interval gas concentration	Sporadically during the campaigns		
Recording interval weather conditions	10 min during all campaigns		

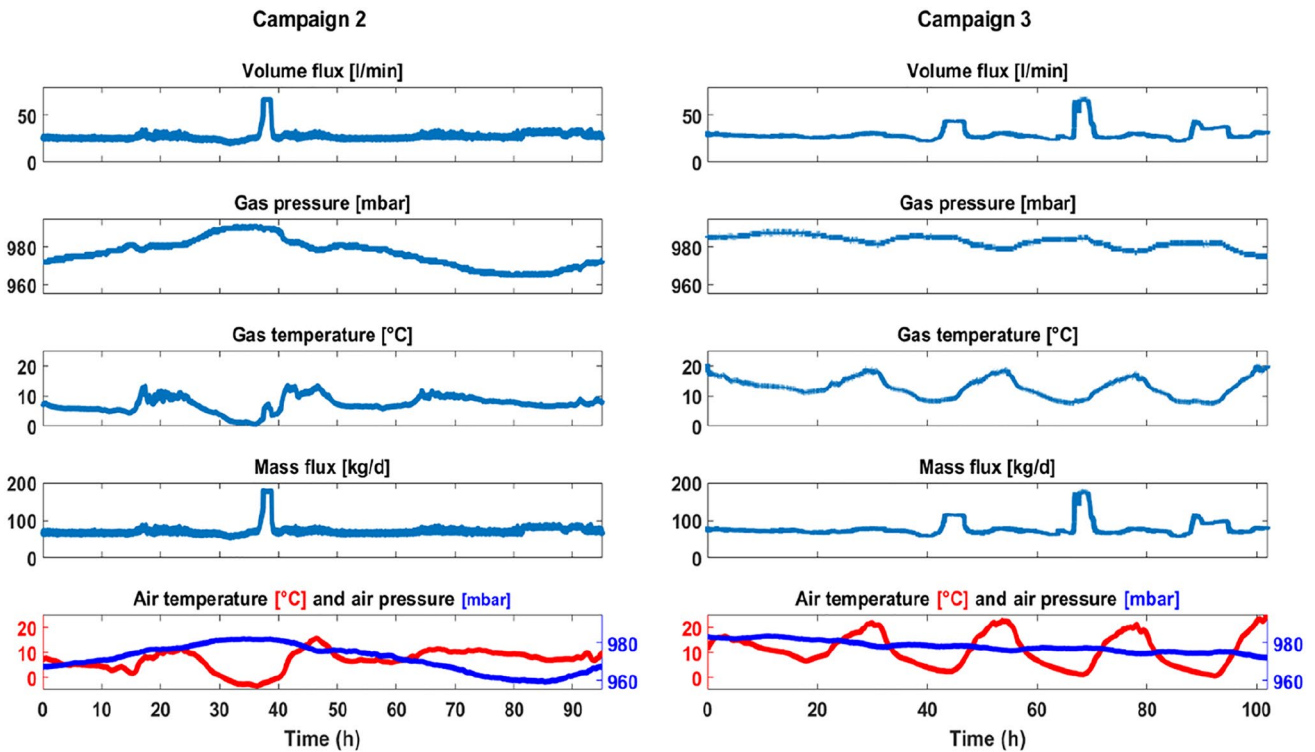


**Fig. 3** Results from field campaigns 2 and 3. Top row shows the gas volume flux in l/min, the second and third row present gas pressure [mbar] and temperature [°C] and the fourth row shows the calculated

CO<sub>2</sub> mass flux [kg/day]. The bottom row shows the meteorological parameters air temperature [°C] and pressure [mbar]

**Table 4** Statistics of the measured and determined parameters during the measurement campaigns ( $\mu$  = arithmetic mean,  $\sigma$  = standard deviation, note: for the statistics measurement artefacts caused by abrupt changes in gas flow velocity were omitted)

Measured parameters	Campaign 1				Campaign 2				Campaign 3			
	Min	Max	$\mu$	$\sigma$	Min	Max	$\mu$	$\sigma$	Min	Max	$\mu$	$\sigma$
Gas flow velocity [m/s]	0.87	1.17	1.02	0.04	0.61	1.07	0.83	0.07	0.6	1.1	0.9	0.07
Volume flux [l/min]	27.8	37.4	32.6	1.4	19.4	34.2	26.4	2.3	20.5	34.0	27.4	1.4
Gas pressure [mbar]	969	978	975	2	965	991	978	7	975	988	983	3
Gas temperature [°C]	5.0	7.7	6.0	0.5	0.5	13.4	7.2	2.8	7.6	20.6	13.4	3.1
CO <sub>2</sub> mass flow rate [kg/d]	73.0	98.6	86.0	3.7	52.5	89.2	69.6	5.4	53.9	85.8	71.1	5.3
Air pressure [mbar]	964	972	969	2.5	959	982	972	7.1	972	983	978	3.0
Air temperature [°C]	1.3	6.6	2.6	1.0	-3.5	15.7	6.9	4.1	0.6	24.4	10.9	6.5

964–972 mbar with a comparable variability. The difference in the measured gas and air pressures lies within the accuracy of the respective sensors and the data showed a very

similar trend with only little variation during the campaign. This indicates a predominant influence of the air pressure on the gas pressure sensor, and it can be concluded that no

back pressure was generated in the hood and no significant changes in exhalation pressure occurred. An almost identical trend of both temperature graphs was also observed, though the gas temperatures are a few degrees higher due to the gas passage through groundwater, but they also show a slight influence of the diurnal cycle of the atmospheric temperature with highest values in the early hours of the afternoon (around 13:00–15:00 h).

The measured gas velocity in the chimney was also comparably constant, the resulting volumetric emission rates varied between approx. 28 L/min and 37 L/min (mean: approx. 33 L/min). Following Eq. (5) and assuming the emanation of pure CO<sub>2</sub> this results in CO<sub>2</sub> mass flow rates ranging between approx. 73 kg/d and 99 kg/d (mean: 86 kg/d). The resulting time series of the CO<sub>2</sub> mass flow rate is comparably constant with a comparably small standard deviation of 3.7 kg/d.

After around 60 h, an abrupt change in gas flow velocity, and accordingly in volumetric and mass flow rates was measured, which however only decreased during the following 6 h. Such jumps were also observed during the other campaigns and are considered an artefact, discussed in more detail later. Therefore, the outlier data was eliminated and not incorporated in the statistical evaluation of the data (Table 4). A similar abrupt change can also be seen after around 15 h in the data, but due to its small magnitude and short duration, it was not considered further.

### Campaign 2

The measurements of the second campaign started in the afternoon and took place over four days without precipitation in early spring during a period with a larger variability of the air temperature (− 3.5 °C and 15.7 °C) than during campaign 1 (Table 4), and with a clear diurnal cycle with maximum temperatures in the hours of the early afternoon. The measured gas temperature data showed a slightly smaller range between 0.5 and 13.4 °C and a smaller variability. Again, the air pressure was slightly lower than the gas pressure, with a similar range and variability. Here also an almost analogous trend was observed between the atmospheric parameters and the gas pressure and temperature although latter showed more fluctuations during this campaign.

The measured gas velocity in the chimney was also comparably constant, the resulting volumetric emission rates varied between approx. 19 L/min and 34 L/min (mean: 26 L/min), which results in CO<sub>2</sub> mass flow rates ranging between approx. 53 kg/d and 90 kg/d (mean: 70 kg/d). The resulting time series of the CO<sub>2</sub> mass flow rate is again comparably constant with a small standard deviation of 5.4 kg/d.

Approx. 25 h after the start of the campaign, the air temperature dropped continuously in the late afternoon to reach a minimum below 0 °C during the night, which resulted also

in a gas temperature of 0.5 °C. During this period, the volume flux showed an abrupt increase and decrease for about approx. 2 h.

### Campaign 3

The measurements of the third campaign started in the late morning and took place over four days without precipitation in late summer. The air temperature showed the highest values of all campaigns (Table 4) with the most pronounced diurnal cycles (0.6–24.4 °C). The cycles are also represented in the gas temperature data, though with higher values on average (7.6–20.6 °C) and less variability. Air and gas pressure values were similar to the previous campaigns but with less variability, and both show a slight, continuous decrease over the entire campaign.

The measured gas velocity in the chimney was also comparably constant, the resulting volumetric flow rates varied between approx. 21 L/min and 34 L/min (mean: 27 L/min), which results in CO<sub>2</sub> mass flow rates ranging between approx. 54 kg/d and 86 kg/d (mean: 71 kg/d). The resulting time series of the CO<sub>2</sub> mass flow rate is again comparably constant with a small standard deviation of 5.3 kg/d.

During this campaign also pronounced sudden increases and decreases appeared in the measurement of the volumetric flow rates (after around 44, 69, and 92 h) which always coincided with minima in gas and air temperature.

In summary, all three campaigns demonstrate the capability of the gas-flow funnel for reliable and reproducible results of CO<sub>2</sub> mass flow rates, and that the gas flow velocity, i.e., volumetric emission, is the driving factor controlling the mass flow rates. Accordingly, air and gas temperatures and pressures have no or only a very minor effect on the resulting gas emission rates. Considering the seasonal changes and associated differences in atmospheric parameters (especially pressure) during the campaigns, it can be concluded that changes in atmospheric conditions had no observable influence on the measured gas flow rates at the site. However, it cannot be excluded that storms or other strong meteorological events might have an impact of the gas emission.

The mean values of volumetric and mass flow rates of all three campaigns are within a close range with average values between 26–33 L/min and 70–86 kg/d, resp. The higher mass flow rates determined on average during the second and third campaign are most likely caused by generally higher gas flow velocities, which are most likely caused by a slightly different placement of the anemometer sensor within the chimney, which was better controlled from the second campaign on.

The estimated CO<sub>2</sub> mass flow rates are consistent with findings from other field sites with comparable CO<sub>2</sub> exhalations, e.g. 0.3–8 kg/d from focused emissions in the area of an inactive volcanic complex in Romania (Kis et al. 2017),



and 1.5–276 kg/d from focused emissions from water and mud pools in the area of Mt. Etna (Giammanco et al. 2007).

### Measurement artefacts

As stated above, changes in atmospheric parameters had in general no or only a very minor impact on the gas volumetric flow rates. However, the diurnal changes in atmospheric temperature are also visible in the gas temperature. It is obvious that the abrupt changes in gas volumetric and mass flow rate in campaigns 2 and 3, which are considered as measurement artefacts, seems to be linked to a significant decrease in the air and gas temperature. To investigate the reasons for these artefacts, several shorter gas flow measurements were performed at the mofette, during which the hot-wire anemometer was removed from the chimney as soon as the flow velocity values increased to the full scale of around 2 m/s. The tests showed repeatedly that water covered the sensor tip of the hot-wire anemometer, resulting in a sensor cooling and leading to unrealistic gas flow velocity values. The water film on the sensor tip most likely formed by condensation of the water–vapor of the emanating gas.

### Conclusions

We presented a simple gas-flow funnel system for the continuous measurement of gas volume and mass fluxes out of focused gas emanation point sources. For the proof-of-concept we tested the system during three field campaigns at a site with advective natural CO<sub>2</sub>-bound emissions associated with a geologic fault in southwestern Germany. The recorded data shows to be comparable and repeatable throughout the three campaigns, but also includes phases of distinct and short-term fluctuations, while no or only very weak effects of changes in atmospheric conditions are obvious in the time series. Only strong temperature drops partly caused a severe influence on the gas flow recording due to a water condensation at the anemometer leading to unrealistic gas flow velocity values. These disturbances occur however only for short periods and can easily be detected due to their clear pattern in the time series of the gas flow velocity.

The general design presented here can easily be applied at sites with focused, advectively driven gas exhalation like volcanic areas, shale-gas seeps, landfills, and open boreholes. The equipment used for our gas-flow funnel is inexpensive, small, light in weight, and easy to build and set up in the field. The sensors and standard acquisition units used with the system usually have only a low power consumption and sufficiently large data storage to acquire time series in extensive field campaigns of several days to even a few weeks. The data acquisition unit we used would even allow for setting up a wireless data transfer and remote control to

reduce the number of field visits during longer measurement campaigns. Also, the sensor array can be simply adapted to other gas compositions and flow velocities. For latter it is however also necessary not only to select an anemometer with an appropriate measurement range, but also to adapt the geometry of the chimney so that gas flow velocities are generated that are in an optimal measurement range, but also no back pressure and turbulent flow is generated in the chimney possible causing skewed gas flow velocities.

The measuring setup can be easily customized to a lot of other site-specific conditions which in our opinion is one of the largest challenges when working at such sites. For example, the size of the exhalation spot can be highly variable, and this can be handled easily by changing the size of the hood. An application in aquatic environments, e.g. in near shore area in lakes or rivers is also possible after adapting the height of the hood, so that it either floats on water or is completely submerged and placed on ground.

**Acknowledgements** The presented work was funded by the German Federal Ministry of Education and Research (BMBF) in the GEOTECHNOLOGIEN program. The financial support of the MONACO project (grant 03G0785K) is gratefully acknowledged. We thank in particular Max-Richard Freiherr von Raßler for support and unlimited access to the field site, and the municipality Starzach. The authors would also like to thank Klaus Faiß and Wolfgang Kürner for their technical support and equipment manufacturing.

**Funding** Open Access funding enabled and organized by Projekt DEAL. This research was funded by Bundesministerium für Bildung und Forschung, Grant no [03G0785K].

### Declarations

**Conflict of interest** None.

**Open Access** This article is licensed under a Creative Commons Attribution 4.0 International License, which permits use, sharing, adaptation, distribution and reproduction in any medium or format, as long as you give appropriate credit to the original author(s) and the source, provide a link to the Creative Commons licence, and indicate if changes were made. The images or other third party material in this article are included in the article's Creative Commons licence, unless indicated otherwise in a credit line to the material. If material is not included in the article's Creative Commons licence and your intended use is not permitted by statutory regulation or exceeds the permitted use, you will need to obtain permission directly from the copyright holder. To view a copy of this licence, visit <http://creativecommons.org/licenses/by/4.0/>.

### References

- Amonette JE, Barr JL (2009) Multi-channel auto-dilution system for remote continuous monitoring of high soil-CO<sub>2</sub> fluxes. Pac Northwest Natl Lab US. <https://doi.org/10.2172/951858>
- Baldocchi DD (2003) Assessing the eddy covariance technique for evaluating carbon dioxide exchange rates of ecosystems: past, present and future. *Glob Change Biol* 9:479–492. <https://doi.org/10.1046/j.1365-2486.2003.00629.x>

- Baldocchi D (2014) Measuring fluxes of trace gases and energy between ecosystems and the atmosphere - the state and future of the eddy covariance method. *Glob Change Biol* 20:3600–3609. <https://doi.org/10.1111/gcb.12649>
- Bigi S et al (2014) Mantle-derived CO<sub>2</sub> migration along active faults within an extensional basin margin (Fiumicino, Rome, Italy). *Tectonophysics* 637:137–149. <https://doi.org/10.1016/j.tecto.2014.10.001>
- Boodoo KS, Trauth N, Schmidt C, Schelker J, Battin TJ (2017) Gravel bars are sites of increased CO<sub>2</sub> outgassing in stream corridors. *Sci Rep* 7:14401. <https://doi.org/10.1038/s41598-017-14439-0>
- Boothroyd IM, Almond S, Qassim SM, Worrall F, Davies RJ (2016) Fugitive emissions of methane from abandoned, decommissioned oil and gas wells. *Sci Total Environ* 547:461–469. <https://doi.org/10.1016/j.scitotenv.2015.12.096>
- Cardellini C, Chiodini G, Frondini F, Granieri D, Lewicki J, Peruzzi L (2003) Accumulation chamber measurements of methane fluxes: application to volcanic-geothermal areas and landfills. *Appl Geochem* 18:45–54. [https://doi.org/10.1016/s0883-2927\(02\)00091-4](https://doi.org/10.1016/s0883-2927(02)00091-4)
- Chiodini G, Frondini F (2001) Carbon dioxide degassing from the Albani Hills volcanic region, Central Italy. *Chem Geol* 177:67–83. [https://doi.org/10.1016/S0009-2541\(00\)00382-X](https://doi.org/10.1016/S0009-2541(00)00382-X)
- Chiodini G, Cioni R, Guidi M, Raco B, Marini L (1998) Soil CO<sub>2</sub> flux measurements in volcanic and geothermal areas. *Appl Geochem* 13:543–552. [https://doi.org/10.1016/s0883-2927\(97\)00076-0](https://doi.org/10.1016/s0883-2927(97)00076-0)
- Coates TW, Flesch TK, McGinn SM, Charmley E, Chen D (2017) Evaluating an eddy covariance technique to estimate point-source emissions and its potential application to grazing cattle. *Agric Meteorol* 234–235:164–171. <https://doi.org/10.1016/j.agrformet.2016.12.026>
- DIN EN 12599 (2012) Ventilation for buildings: test procedures and measurement methods to hand over air conditioning and ventilation systems. *Germ Inst Stand*. <https://doi.org/10.31030/1890806>
- Dixon T, Romanak KD (2015) Improving monitoring protocols for CO<sub>2</sub> geological storage with technical advances in CO<sub>2</sub> attribution monitoring. *Int J Greenh Gas Control* 41:29–40. <https://doi.org/10.1016/j.ijggc.2015.05.029>
- Dumortier P, Aubinet M, Lebeau F, Naiken A, Heinesch B (2019) Point source emission estimation using eddy covariance: validation using an artificial source experiment. *Agric for Meteorol* 266–267:148–156. <https://doi.org/10.1016/j.agrformet.2018.12.012>
- El Hachem K, Kang M (2022) Methane and hydrogen sulfide emissions from abandoned, active, and marginally producing oil and gas wells in Ontario. *Can Sci Total Environ*. <https://doi.org/10.1016/j.scitotenv.2022.153491>
- Elío J, Ortega MF, Chacón E, Mazadiego LF, Grandia F (2012) Sampling strategies using the “accumulation chamber” for monitoring geological storage of CO<sub>2</sub>. *Int J Greenh Gas Control* 9:303–311. <https://doi.org/10.1016/j.ijggc.2012.04.006>
- Etiopie G, Klusman RW (2002) Geologic emissions of methane to the atmosphere. *Chemosphere* 49:777–789. [https://doi.org/10.1016/S0045-6535\(02\)00380-6](https://doi.org/10.1016/S0045-6535(02)00380-6)
- Evans WC et al (2002) Tracing and quantifying magmatic carbon discharge in cold groundwaters: lessons learned from Mammoth Mountain. *USA J Volcanol Geotherm Res* 114:291–312. [https://doi.org/10.1016/s0377-0273\(01\)00268-2](https://doi.org/10.1016/s0377-0273(01)00268-2)
- Feitz A et al (2018) The Ginninderra CH<sub>4</sub> and CO<sub>2</sub> release experiment: an evaluation of gas detection and quantification techniques. *Int J Greenh Gas Control* 70:202–224. <https://doi.org/10.1016/j.ijggc.2017.11.018>
- Forde ON, Cahill AG, Beckie RD, Mayer KU (2019) Barometric-pumping controls fugitive gas emissions from a Vadose Zone natural gas release. *Sci Rep* 9:9. <https://doi.org/10.1038/s41598-019-50426-3>
- Gal F, Kloppmann W, Proust E, Humez P (2018) Gas concentration and flow rate measurements as part of methane baseline assessment: Case of the Fontaine Ardente gas seep Isere, France. *Appl Geochem* 95:158–171. <https://doi.org/10.1016/j.apgeochem.2018.05.019>
- Gal F, Proust E, Kloppmann W (2019) Towards a better knowledge of natural methane releases in the French Alps: a field approach. *Geofluids* 2019:6487162. <https://doi.org/10.1155/2019/6487162>
- Giammanco S, Parello F, Gambardella B, Schifano R, Pizzullo S, Galante G (2007) Focused and diffuse effluxes of CO<sub>2</sub> from mud volcanoes and mofettes south of Mt. Etna (Italy). *J Volcanol Geotherm Res* 165:46–63. <https://doi.org/10.1016/j.jvolgeores.2007.04.010>
- Heggie AC, Stavropoulos B (2018) Passive diffusive flux chambers – a new method to quantify vapour intrusion into indoor air. *Environ Sci* 20:523–530. <https://doi.org/10.1039/C7EM00569E>
- Holloway S, Pearce JM, Hards VL, Ohsumi T, Gale J (2007) Natural emissions of CO<sub>2</sub> from the geosphere and their bearing on the geological storage of carbon dioxide. *Energy* 32:1194–1201. <https://doi.org/10.1016/j.energy.2006.09.001>
- Jones DG et al (2014) Monitoring of near surface gas seepage from a shallow injection experiment at the CO<sub>2</sub> field lab, Norway. *Int J Greenh Gas Control* 28:300–317. <https://doi.org/10.1016/j.ijggc.2014.06.021>
- Jovanov D, Vujić B, Vujić G (2018) Optimization of the monitoring of landfill gas and leachate in closed methanogenic landfills. *J Environ Manag* 216:32–40. <https://doi.org/10.1016/j.jenvman.2017.08.039>
- Jung NH, Han WS, Han K, Park E (2015) Regional-scale advective, diffusive, and eruptive dynamics of CO<sub>2</sub> and brine leakage through faults and wellbores. *J Geophys Res-Solid Earth* 120:3003–3025. <https://doi.org/10.1002/2014jb011722>
- Kang M et al (2014) Direct measurements of methane emissions from abandoned oil and gas wells in Pennsylvania. *Proc Natl Acad Sci* 111:18173. <https://doi.org/10.1073/pnas.1408315111>
- Kis B-M, Ionescu A, Cardellini C, Harangi S, Baciu C, Caracausi A, Viveiros F (2017) Quantification of carbon dioxide emissions of Ciomadul, the youngest volcano of the Carpathian-Pannonian Region (Eastern-Central Europe, Romania). *J Volcanol Geotherm Res* 341:119–130. <https://doi.org/10.1016/j.jvolgeores.2017.05.025>
- Levintal E, Lensky NG, Mushkin A, Weisbrod N (2018) Pipes to earth’s subsurface: the role of atmospheric conditions in controlling air transport through boreholes and shafts. *Earth Syst Dyn* 9:1141–1153. <https://doi.org/10.5194/esd-9-1141-2018>
- Levintal E, Dragila MI, Zafirir H, Weisbrod N (2020) The role of atmospheric conditions in CO<sub>2</sub> and radon emissions from an abandoned water well. *Sci Total Environ* 722:1857. <https://doi.org/10.1016/j.scitotenv.2020.137857>
- Lewicki JL, Evans WC, Hilley GE, Sorey ML, Rogie JD, Brantley SL (2003) Shallow soil CO<sub>2</sub> flow along the San Andreas and calaveras faults. *Calif J Geophys Res*. <https://doi.org/10.1029/2002J B002141>
- Lübben A, Leven C (2018) The Starzach site in Southern Germany: a site with naturally occurring CO<sub>2</sub> emissions recovering from century-long gas mining as a natural analog for a leaking CCS reservoir. *Environ Earth Sci* 77:316. <https://doi.org/10.1007/s12665-018-7499-y>
- Moncrieff JB et al (1997) A system to measure surface fluxes of momentum, sensible heat, water vapour and carbon dioxide. *J Hydrol* 188:589–611
- Neeper DA (2003) Harmonic analysis of flow in open boreholes due to barometric pressure cycles. *J Contam Hydrol* 60:135–162. [https://doi.org/10.1016/S0169-7722\(02\)00086-4](https://doi.org/10.1016/S0169-7722(02)00086-4)
- O’Dwyer M, Padgett MJ, McGonigle AJ, Oppenheimer C, Inguaggiato S (2003) Real-time measurement of volcanic H<sub>2</sub>S and SO<sub>2</sub> concentrations by UV spectroscopy. *Geophys Res Lett*. <https://doi.org/10.1029/2003GL017246>

- Sauer U, Schuetze C, Leven C, Schloemer S, Dietrich P (2014) An integrative hierarchical monitoring approach applied at a natural analogue site to monitor CO<sub>2</sub> degassing areas. *Acta Geotechn* 9:127–133. <https://doi.org/10.1007/s11440-013-0224-9>
- Scheutz C, Kjeldsen P (2019) Guidelines for landfill gas emission monitoring using the tracer gas dispersion method. *Waste Manag* 85:351–360. <https://doi.org/10.1016/j.wasman.2018.12.048>
- Schuetze C, Vienken T, Werban U, Dietrich P, Finizola A, Leven C (2012) Joint application of geophysical methods and direct push-soil gas surveys for the improved delineation of buried fault zones. *J Appl Geophys* 82:129–136. <https://doi.org/10.1016/j.jappgeo.2012.03.002>
- Shimoike Y, Kazahaya K, Shinohara H (2002) Soil gas emission of volcanic CO<sub>2</sub> at Satsuma-Iwojima volcano. *Jpn Earth Planets Space* 54:239–247. <https://doi.org/10.1186/BF03353023>
- Sorey ML, Evans WC, Kennedy BM, Farrar CD, Hainsworth LJ, Hausback B (1998) Carbon dioxide and helium emissions from a reservoir of magmatic gas beneath Mammoth Mountain. *Calif J Geophys Res* 103:15303–15323. <https://doi.org/10.1029/98JB01389>
- Steinitz G, Piatibratova O, Barbosa SM (2007) Radon daily signals in the Elat Granite, southern Arava. *Israel J Geophys Res*. <https://doi.org/10.1029/2006JB004817>
- Symonds RB, Rose WI, Bluth GJS, Gerlach TM (2018) Volatiles in Magmas. In: Michael RC, John RH (eds) Chapter 1 volcanic-gas studies: methods, results, and applications. De Gruyter, Berlin, pp 1–66. <https://doi.org/10.1515/9781501509674-007>
- Werner C, Kelly PJ, Doukas M, Lopez T, Pfeffer M, McGimsey R, Neal C (2013) Degassing of CO<sub>2</sub>, SO<sub>2</sub>, and H<sub>2</sub>S associated with the 2009 eruption of Redoubt Volcano. *Alaska J Volcanol Geotherm Res* 259:270–284. <https://doi.org/10.1016/j.jvolgeores.2012.04.012>
- Zafir H, Ben Horin Y, Malik U, Chemo C, Zalevsky Z (2016) Novel determination of radon-222 velocity in deep subsurface rocks and the feasibility to using radon as an earthquake precursor. *J Geophys Res* 121:6346–6364. <https://doi.org/10.1002/2016JB013033>
- Zafir H, Barbosa S, Levintal E, Weisbrod N, Ben Horin Y, Zalevsky Z (2020) The impact of atmospheric and tectonic constraints on radon-222 and carbon dioxide flow in geological porous media: a dozen-year research summary. *Front Earth Sci* 8:28. <https://doi.org/10.3389/feart.2020.559298>

**Publisher's Note** Springer Nature remains neutral with regard to jurisdictional claims in published maps and institutional affiliations.